Proceedings of the Institution of Mechanical Engineers, Part D: Journal of Automobile Engineering
Volume 234, Issue 1, January 2020, pp. 85-97
DOI:10.1177/0954407019838642

Experimental investigation of the cooling characteristics of a monobloc cast iron brake disc with fingered hub

Marko Tirovic*, Stergios Topouris and Glenn Sherwood

Cranfield University, School of Aerospace, Transport and Manufacturing,

College Road, Cranfield, MK43 0AL, United Kingdom

* *Corresponding author: m.tirovic@cranfield.ac.uk*

Abstract

The paper compares heat dissipation characteristics of two interchangeable ventilated brake discs, a standard solid hub and a newly developed fingered hub version, both single piece cast designs. The tests were conducted on a specially developed Thermal Flow Rig, which enables disc induction heating to 450°C and cooling for a range of rotational and air speeds, in parallel and angular cross flow. The Rig facilitated very accurate and repeatable experiments to be conducted for numerous combinations of operating conditions. From the recorded cooling curves average heat transfer coefficients for convection and radiation were extracted and the results also presented in a generic form, using Nusselt numbers. The fingered design demonstrated superior convective heat dissipation, with the improvements varying depending on the rotational speed, air cross flow velocity and angle, as well as disc temperature. The gains were ranging from 3.5% to over 20%. The fingered design is 8.5% lighter and being a single piece cast disc it remains inexpensive to mass produce.

Keywords: Brake Disc, Heat Dissipation, Convective Cooling, Emissivity, Thermal Flow Rig, Flow visualisation

NOMENCLATURE

Symbol	Description	Unit
A_{rad}	Radiative heat dissipation disc area	[m^2]
A_w	Total disc wetted area	[m^2]
c_p	Specific heat of disc material (grey iron)	[J/kgK]
h_{conv}	Average convective heat transfer coefficient	[W/m^2K]
h_{rad}	Average radiative heat transfer coefficient	[W/m^2K]
h_{tot}	Total average heat transfer coefficient	[W/m^2K]
l	Characteristic length	[m]
m	Disc mass	[kg]
Nu	Nusselt Number	-
Re	Reynolds Number	-
Re_t	Crossflow Reynolds Number	-
Re_ω	Rotational Reynolds Number	-
R_o	Outer Radius	[m]
T_d	Average disc temperature during time period t_1 to t_2	[K]
T_{d1}	Disc temperature at the time t_1	[K]
T_{d2}	Disc temperature at the time t_2	[K]
T_∞	Ambient air temperature	[K]
U	Air velocity	[m/s]
t	Time	[s]
ε	Disc surface emissivity	-
κ	Thermal conductivity of air	[W/mK]
ν	Kinematic viscosity of air	[m^2/s]
ω	Angular velocity	[rad/s]
ρ	Air density	[kg/m^3]
σ	Stefan-Boltzmann constant (5.67×10^{-8})	[W/m^2K^2]

1. Introduction

1.1. Background, Aims and Objectives

The development of fingered disc design was motivated by the need to reduce vehicle unsprung mass and improve brake disc cooling characteristics. Similar, 'fingered' type discs usually have several parts, requiring accurate machining and assembling which considerably increases the cost. The approach presented here is aiming at a single piece (monobloc) cast iron disc. As such, the design should be competitively priced, still offering substantial benefits in terms of lower mass and rotating inertia, as well as better heat dissipation. The main problem in generating such a design for passenger cars is related to the structural integrity of the fingered hub. The authors have demonstrated that such design is possible to establish, as detailed in [1]. There are however limitations, a) the vehicle needs to be light and corresponding maximum braking torque relatively low and b) the top hat offset needs to be small, resulting in a relatively 'shallow' disc design. The vehicle selected was Lotus Elise S2 which has such a disc design (identical for both axles). This is a high performance vehicle but still at a low cost. The vehicle has considerable followers and is widely used on the road as well as on the racetrack. The aftermarket offering of bespoke performance parts is high. Consequently, low cost solutions are very desirable, in particular when offering further advantages in reduced mass and rotary inertia, in addition to better cooling. The original disc is presented in Figure 1a, and fingered design in Figure 1b, with the main characteristics summarised in Table 1. The fingered design was created by machining pockets in the disc hub, in order to validate structural and cooling aspects in a short time and at low cost.

a) **b)**

Figure 1 Brake discs: **a)** The original, solid hub design; **b)** New, fingered hub design

In this article, determination of the heat dissipation and flow characteristics was to be conducted experimentally, aiming at the comparison of the two discs cooling characteristics. For that purpose, a special Thermal Flow Rig was designed, manufactured and commissioned. This facilitated cooling tests and flow studies to be performed for the range of rotational speeds, cross air velocities and angles. Controlled environment enabled repeatable tests and reliable results. The findings are to be presented in a generic form using Nusselt numbers, enabling their wider use in brake temperature predictions.

Characteristics	Original design *(Figure 1a)*	Fingered design *(Figure 1b)*
Outer Diameter	288 mm	288 mm
Inner Diameter	182 mm	182 mm
Thickness	26 mm	26 mm
Type and number of vanes	Curved, 37	Curved, 37
Mass	6.00 kg	5.50 kg
Convective heat dissipation area	0.2495 m^2	0.2372 m^2
Radiative heat dissipation area	0.1321 m^2	0.1217 m^2

Table 1 Characteristics of brake discs studied

1.2. Literature review

Heat is dissipated from brake components by all three modes; conduction, convection and radiation, with each of the modes being defined by a very different physical law. Furthermore, the operational and environmental aspects discussed above influence the three modes in different ways. The temperatures measured represent the 'final outcome' of all three heat dissipation modes. Small variation in any of the modes may not drastically change measured temperatures as the contribution of the other two heat dissipation modes will increase. The uncertainties are considerable, and any models created should be supported with numerous temperature measurements for different duties. It is very important to gradually increase the complexity of both the tests and models. A number of publications deal with experimental studies of heat dissipation from road vehicle brakes, with the fundamentals established by Newcomb [2] for heat dissipation from vehicle disc brakes. However, starting from the very fundamentals, Wagner [3] was the first author publishing the analytical approach in disc flow and heat dissipation from solid discs rotating in still air. He expressed the results in a generic form, as Nusselt number as a function of rotational Reynold number, the form which has been adopted ever since and used by the authors of this article (e.g. Equation 7). Cobb and Saunders [4] continued the research in the same area experimentally and concluded that numerous studies yield somewhat higher Nusselt numbers than theoretically predicted by Wagner [3]. They also concluded that the transition of the flow from predominantly laminar to turbulent occurs for rotational Reynolds numbers over 240,000, which is less than half of the value originally quoted by Wagner at 500,000. Further studies by Richardson and Saunders [5] demonstrated that the accuracy can be improved by the inclusion of the Grashof number. Noyes and Vickers [6] used numerical methods, which enabled accurate inclusion of the radiative heat dissipation and validated the results experimentally. The average value for disc brake emissivity used by the authors of $\varepsilon = 0.55$ is still widely used by many authors. Morgan and Dennis [7] studied discs rotating in a cross flow and expanded the initial formula established by Wagner [3] by including the ratio of Reynolds cross flow and rotational numbers. This approach has been widely accepted and used by the authors of this article (e.g. Equation 8). Limpert [8] and Sisson [9] addressed

ventilated discs and tried to separate the heat dissipation from disc faces and ventilation channels. Although their work is of a high quality, the findings are limited to the discs of similar design and size, number of channels and type and length of vanes. The flow within ventilating channels, in particular in cross flow is far too complicated for derivation of any generic relationships. Convective heat dissipation is the dominant mode of heat dissipation in most braking duties but the influence of the other two modes, conduction and radiation, must be accurately accounted for in order for the convective heat dissipation predictions to be accurate. Disc contact areas with the mounting flange can be insulated and temperatures monitored for reducing and monitoring conductive heat losses. However, radiative heat losses are difficult to accurately measure as disc emissivity is influenced by numerous parameters and varies with temperature. In that sense, a big step forward has been made recently by Dufrenoy et al. [10] offering an advanced solution in measuring disc surface emissivity. Whatever the approach in measuring temperatures and associated parameters, uncertainties in dealing with test data are of paramount importance. This is probably best addressed by Moffat [11].

Numerous authors investigated heat transfer from brakes using numerical methods, Computational Fluid Dynamics (CFD) and Finite Element (FE) methods. Though a lot of that work is of good quality and deserves attention, the results are of limited generic values as they relate to the specific designs, installations and operating conditions. It is worth mentioning the work related to disc brake design and materials published by Grieve et al. [12], with Tang et al. [13] relating thermal aspects with brake judder. Finally, Stevens [14] studied heat dissipation from stationary commercial vehicle disc brake using analytical and numerical models and experiments. The analytical models and experimental work, including uncertainty analyses, presented by Stevens and Tirovic [15] are of particular interest, demonstrating substantial complexities and variations.

In addition to the convection and radiation, it should be pointed out that conduction can play an important role in heat dissipation from brakes. Tirovic and Voller [16] demonstrated that accurate predictions for heat dissipation form a commercial vehicles brake disc are possible. Furthermore, Teimourimanesh et al. [17] established the considerable influence of the rails in conductive cooling of railway tread brakes.

Following from the above considerations, the authors have adopted a step by step approach in gradually increasing the complexity of the test conditions for studying heat dissipation from the two disc designs. Initially, the discs were tested when rotating in still air, then the experiments were conducted in parallel and angular cross flow in the Thermal Flow Rig, with further details are given by Topouris [18].

2. Experimental facility: Thermal Flow Rig

This facility was developed and installed in Cranfield University. The CAD model is shown in Figure 2 (side and top views), indicating three main sub-assemblies, the flow channel, disc rotating and heating assembly and fan unit. The position of the flow straightener and ‘Middle plane’ are also indicated, with

Table 2 summarising the main operational characteristics of the Thermal Flow Rig, following the commissioning phase.

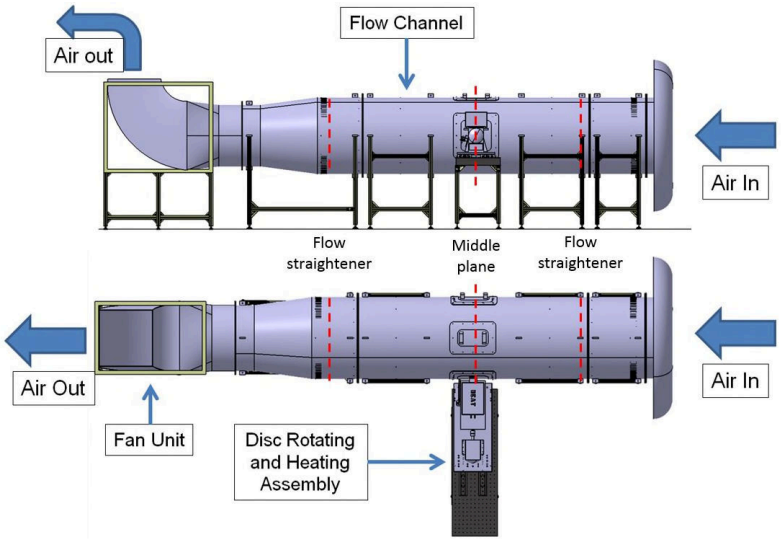

Figure 2 Thermal Flow Rig

Flow channel inner diameter	1,000 mm
Air velocity range	2.5 – 13.5 m/s
Fan motor power	22 kW
Fan propeller: Number of blades / angle	9 / 12º
Maximum disc rotational speed	2,643 rpm
Steering knuckle maximum angles	-28º to 25º
Outer disc diameter	Up to 434 mm
Disc mass	Up to 35 kg
Maximum induction heater power	15 kW
Maximum heating temperature (typical)	450ºC to 500 ºC

Table 2 Thermal Flow Rig characteristics

2.1. Flow Channel and Fan Assembly

The Flow Channel, together with the Fan Unit are shown in Figure 3a, where, in the direction of the air flow, 1 is the intake bellmouth, 2 intake segment, 3 working segment, 4 conical segment, 5 fan unit, 6 adapter plate and 7 exhaust outlet. The length of the working segment 3 is 2,600mm, with aluminium honeycomb flow straighteners placed just before and after this segment. The total length of the components 1 to 4 is 5,750 mm. The Rig is a 'through flow' type, hence the bell mouth intake is located next to a large door which is kept opened during operation (Figure 3b).

a) **b)**

Figure 3 Flow Channel

a) Side view and **b)** Front view (bellmouth)

In order to obtain accurate results and ensure repeatability of the tests, it is vital to ensure good quality flow in the working segment, in particular in middle plane (see Figure 2). The flow channel was commissioning following the ASHRAE Standard 111-1988, confirming very uniform air flow up to about 80 mm from the wall for the highest air speed. At the disc position (middle plane in Figure 2), there was practically no measureable air speed change within the 840mm cross section diameter in the middle of 1,000mm channel diameter.

2.2. Disc Rotating and Heating Assembly

Disc Rotating and Heating Assembly is shown in Figure 4a, with the rubbing thermocouple detail shown in Figure 4b. The assembly consists of a Table 1, with the Base Plate 2 mounted on the table via sliders, enabling accurate axial positioning. Axle assembly 3 gives structural support to all rotating parts, connecting to a steering knuckle 4 at the disc end, with the electric motor 5 placed at the other end. The disc 6 is thermally insulated on both sides, using 15mm thick peek plastic inserts. Induction heater head 7 is connected to coil 8. Figure 4b details the disc, showing 3 rubbing thermocouples placed on one friction surface of the disc.

Figure 5a shows the part of the Disc Rotating and Heating Assembly inside the Flow channel. The photograph is taken from the intake (bellmouth) side, after the first flow straightener. The access hatch on the right hand side can be seen. In Figure 5b, this hatch has been removed to get better view of the disc tested. In addition to the disc, 3 rubbing thermocouples can be clearly seen, as well as the induction heating coil. This coil is manufactured from a special copper tube, enabling high voltage, high frequency current to be transmitted for disc heating. Constant flow of cold water is necessary and, since the disc can be steered, special water tight and electrically conducting flexible hoses have been used. Induction

heating system based on Ambrell ISM HF 15 170 control unit, heating up the disc to over 450°C in less than 10 minutes.

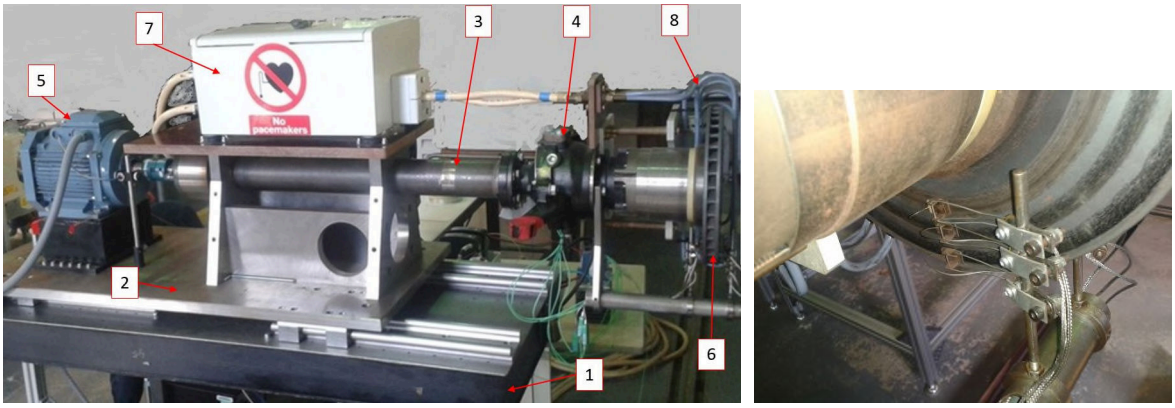

a) **b)**

Figure 4: **a)** Disc rotating and heating assembly and **b)** Disc and thermocouples detail

a) **b)**

Figure 5 Disc in the Flow channel: **a)** Front view and **b)** Side view (right hand hatch removed)

2.3. Instrumentation

The instrumentation was based on National Instruments (NI) CompactRIO 9022 measuring and data logging system, connected to a PC. As shown in Figures 4 and 5, rubbing thermocouples (K Type) were used, the arrangement common in automotive industry. In the commissioning phase, additional rubbing thermocouples with graphite tips were placed on the large cylindrical hub surface, to assess conductive heat transfer into the rotating assembly. Numerous tests demonstrated that conductive heat transfer is very low and can be neglected, as the temperature change during disc heating and cooling is below 1°C. To investigate the 'worst case scenario', the insulating peek flanges were replaced by high conductivity aluminium flanges. The change in temperature was below 2°C with no detectable difference in recorded cooling curves. Additional, frictionally generated heat and thermal contact resistances at thermocouple/disc contact were also investigated but due to low interface pressure and large contact

areas, again there was no influence on the results. Ambient air temperature was measured using a probe type thermocouple. Air temperature and humidity were also measured using Tempatron DP thermometer/hygrometer. Pitot tubes (8mm diameter, different lengths) connected to CMR P-Sensor were used to measure air velocity in the Flow Channel. Cheery EP GS100502 hall sensor was used to measure disc rotational speed. Detailed uncertainty analysis for a very similar set up is presented in [14].

3. Operational Procedure

3.1. Obtaining cooling curves

The operational procedure has three distinctive phases:

a) Heating period

The disc is rotating at low speed (~ 100 rpm) and the induction heater is turned on until disc average temperature of just over 450°C was reached.

b) Soaking period

The induction heater is turn off and the disc is continuing to rotate at low speed (~ 100 rpm) for several minutes in order to equalise the temperatures. Then, disc rotational and air flow speeds are brought to the required values.

c) Cooling down period

The disc is typically cooled down to under 100 °C. Disc surface temperatures logged during this period are the actual 'cooling curves' for the specific test conditions and used to calculate average heat transfer coefficients.

Figure 6 shows disc surface temperatures for the disc rotating at 398 rpm in still air during soaking and cooling periods. The disc was heated to around 500 °C and the 6 rubbing thermocouples initially show somewhat different temperatures, with prefix 'I' referring to the inboard and 'O' to the outboard disc friction surface. It can be noticed that the temperatures at the surfaces are somewhat different at the beginning but can be safely averaged and within 5 minutes, all 6 thermocouples show practically identical temperature of approx. 300 °C. As the disc is heated inductively, there are no hot spots, contact debris, pad deposits or similar irregularities on the disc surface associated with frictional heating. However, the heating rate is higher at disc OD, hence the temperatures are higher at the end of the heating period.

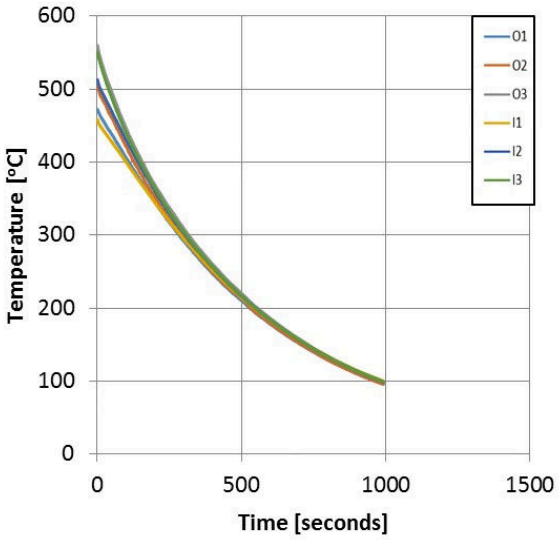

Figure 6 Cooling curves

3.2. Calculating average heat transfer coefficients

During the cooling period there is no heat input, therefore, the average total heat transfer coefficient h_{tot} during the period t_1 to t_2 be can defined as:

$$h_{tot} = -ln\left(\frac{T_{d2} - T_\infty}{T_{d1} - T_\infty}\right)\frac{mc_p}{A_w(t_2 - t_1)} \tag{1}$$

where:

T_{d2} is disc temperature at the time t_2;

T_{d1} is disc temperature at the time t_1;

T_∞ is ambient temperature;

m is disc mass;

c_p is specific heat of disc material (grey iron);

A_w is total disc wetted area.

The average coefficient of heat transfer due to radiation during the period t_1 to t_2 can be defined as:

$$h_{rad} = \varepsilon\sigma\left(\frac{A_{rad}}{A_w}\right)\left(\frac{T_d^4 - T_\infty^4}{T_d - T_\infty}\right) \tag{2}$$

where:

ε is disc surface emissivity;

σ is Stefan-Boltzmann constant;

A_{rad} is radiative heat dissipation disc area;

T_d is average disc temperature during the period $(t_2 - t_1)$.

Accordingly, the average convective heat transfer coefficient, for the period $(t_2 - t_1)$, can be calculated as:

$$h_{conv} = h_{tot} - h_{rad} \quad (3)$$

The temperature differences $(T_{d2} - T_{d1})$ at around 50°C are considered most suitable for calculations, providing reliable disc surface temperatures and sufficiently short periods to account for highly non-linear influence of radiative heat losses.

To maximise the accuracy of the calculated heat transfer coefficients, temperature dependent values were used for specific heat capacity c_p of the disc material (grey cast iron). With regards to emissivity, the values for each disc were identified by comparing the logged temperature from each of the six rubbing thermocouples and then adjusting the emissivity setting on a *Flir i3* thermal imaging camera in order to achieve same temperature readings. Inevitably, the identified emissivity values were an average of the different local emissivity values that exist on the disc areas. It is interesting to point out that the emissivity values were largely temperature independent but somewhat different values were established for the solid and fingered hub discs, being $\varepsilon = 0.80$ and $\varepsilon = 0.82$ respectively. As mentioned earlier on, disc surfaces were corroded, following repeated heating and cooling cycles.

3.3. Calculating Reynolds and Nusselt numbers

Convective heat transfer coefficients are important for predicting disc temperatures using a variety of models, from 1D lumped mass to 3D Finite Element models. It has long been established in brake thermal analyses that the boundary conditions (i.e. heat transfer coefficients) are much more important for reliable temperature predictions than model complexities. Another important use of experimentally derived heat transfer coefficients is their comparisons with CFD predictions.

In deriving heat transfer coefficients for a specific disc design and air flow conditions, it is also important to establish a more generic relationships, enabling extrapolations of the values for different air speeds and disc sizes of an identical or similar design. This also relates to the comparisons of the own findings with those from literature. Reynolds and Nusselt numbers play vital role in such analyses and the fundamentals will be presented here. It should be pointed out that Prandtl, Grashof and Rayleigh numbers can be also helpful when studying disc cooling, in particular related to natural convection [14]. However, for relatively high disc rotational and air velocities used here, the contribution of the natural convection to disc cooling is very low and it is sufficient to use Reynolds and Nusselt numbers.

Reynolds number is actually a ratio between the forces of inertia and viscosity. In the analysis of the disc rotating in still air, Reynolds (rotational) number is equal to:

$$Re_{\omega} = \frac{\omega R_o^2}{\nu} \quad (4)$$

where:

ω is disc angular velocity;

R_o is outer disc radius;

ν kinematic viscosity of air.

If a disc is subjected to a cross flow, Reynolds (cross flow) number is defined as:

$$Re_t = \frac{UR_o}{\nu} \tag{5}$$

where:

U is air speed.

Various authors quote different values of the Reynolds numbers when the flow becomes predominantly turbulent but most sources state the value of 240 000, as initially established by Cobb and Saunders [4].

The Nusselt number, or criterion of heat transfer, is a dimensionless number that distinguishes the heat transfer process at the "wall-fluid" boundary. In other words, it represents the ratio of convective and conductive heat transfer between the solid surface boundary and the fluid that flows across its thickness in the direction normal to the surface of the solid.

$$Nu = \frac{h_{conv} l}{\kappa} \tag{6}$$

where:

h_{conv} is convective heat transfer coefficient;

l is the characteristic length, i.e. disc outer radius R_o;

κ thermal conductivity of air.

For brake disc analysis, it is commonly accepted that Nusselt number is a function of Reynolds numbers, depending on the flow conditions. For disc rotating in still air, the relationship with rotational Reynolds number Re_ω is expressed in the form initially established by Wagner [3]

$$Nu = aRe_\omega^b \tag{7}$$

where terms a and b can be calculated from experimental results.

For disc rotating in air cross flow, the relationship with rotational Reynolds number Re_ω and cross flow Reynolds number Re_t is expressed in the form initially established by Morgan and Dennis [7]

$$Nu = aRe_\omega^b \left[\frac{Re_t}{Re_\omega}\right]^c \tag{8}$$

where terms a, b and c are determined experimentally.

4. Discs rotating in still air

When conducting cooling tests in still air, the disc was heated and cooled outside the flow channel, in a large draft-free laboratory. It would take too much space to present all the result obtained, hence it is considered most appropriate to select the temperature of 275°C, which is approximately in the middle of the temperature range to which most discs are exposed. The results shown in Figure 7 clearly demonstrate much better cooling characteristics of the fingered disc design. There is an improvement of over 20% throughout the speed range from 437 to 2219 rpm (corresponding to vehicle speeds of 50 to 250 km/h).

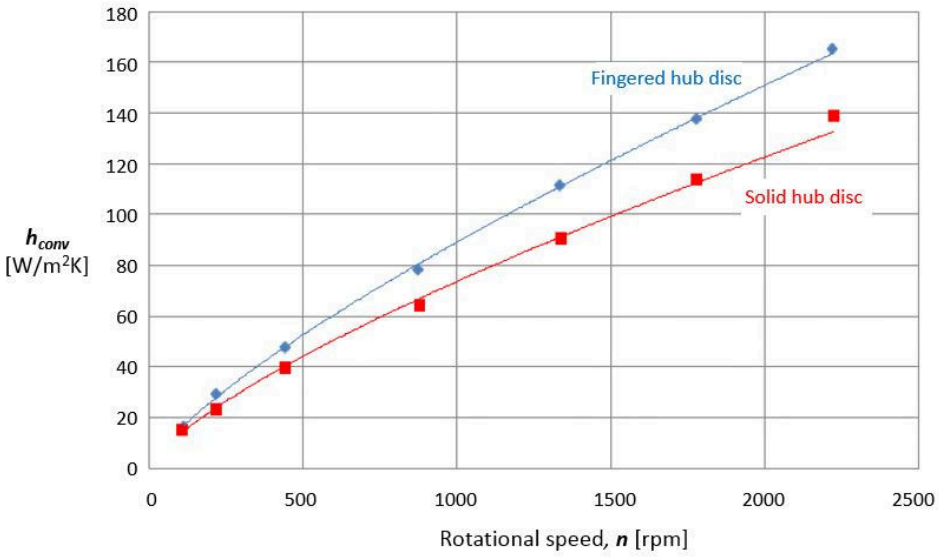

Figure 7 Change of the convective heat transfer coefficients for solid and fingered disc with rotational speed at 275°C

Using Nusselt numbers approach, Equation (7), the terms *a* and *b* are graphically presented in Figure 8. The results cannot be as vividly interpreted as the graphs shown in Figure 7 but are very useful in calculating convective heat transfer coefficients for a range of test conditions. It can be noticed that two discs have similar values for terms *a* and *b* at lower temperatures but the differences increase with the increase in temperatures. When compared to the fingered disc, term *a* increases much more rapidly with temperature for the solid hub disc. Term *b* is reducing by about 10% for the solid but only about 2% for the fingered design. This is probably the consequence of relatively small gap between the inner disc diameter and top hat section of the solid disc, as the air is trying to 'squeeze' through at higher speeds. Fingered design has no such obstacles as the air can be drawn from both sides. Terms *b* are close to the theoretical value 0.8 (for both discs) quoted by many authors. The lowest Re_ω value is approx. 4,100, for the disc rotating at the lowest speed and highest temperature, with the highest value being 175,500 for the highest speed and lowest disc temperature. The latter is still within laminar range, considering that the flow becomes predominantly turbulent at $Re_\omega \approx 240{,}000$.

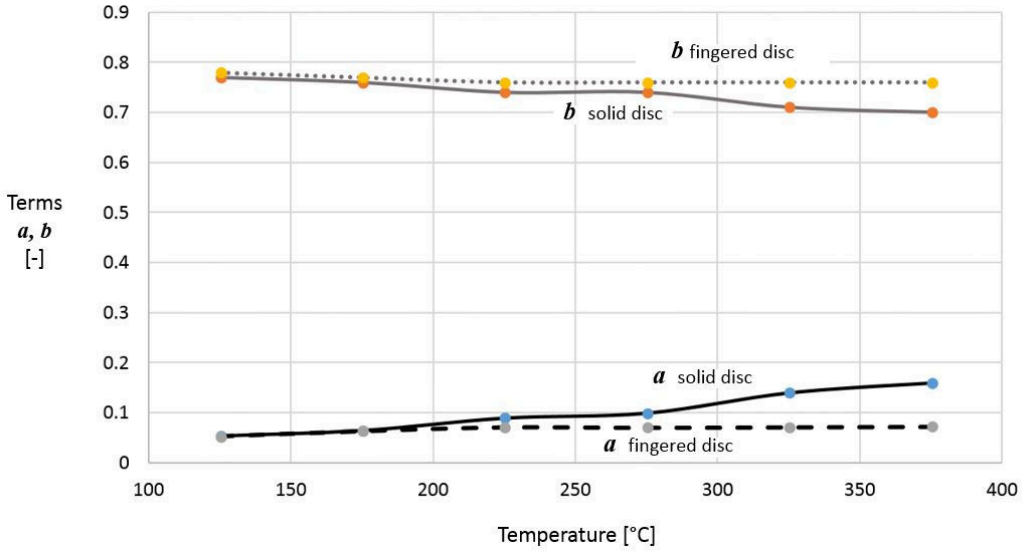

Figure 8 Cooling characterisation in still air: Terms ***a*** and ***b*** for solid and fingered disc (Equation 7)

5. Discs rotating in a parallel cross flow

These tests were conducted in the flow channel where air flow velocity can be varied independently from disc rotational speed. In most road vehicles the *'equivalent'* air cross flow velocity around the disc is lower than the vehicle speed. In other terms, if the vehicle is travelling at 100 km/h, the *equivalent* cross flow air velocity at brakes is lower, typically about half of that speed (or lower), i.e. around 50 km/h. This is due to the restricted air intake around the wheels and brakes, which can be influenced by modifying the dust shields/splash plates. Special air scoops can be particularly effective and are often used in racing vehicles. Following these considerations, the tests were conducted for disc rotational speeds proportional to air velocity, and additionally for rotational speeds 1.5 times higher, twice higher and three times higher. These effects are particularly well encountered by Son et al. [19] investigating a brake cooling scoop for a passenger car.

The results, in the form of calculated convective heat transfer coefficient are summarised in Figure 9, for 275°C. The general trend is similar for both discs, with the convective heat transfer coefficients increasing approximately linearly with the air speed. As expected, increase of rotational disc speed improves the cooling but the effect is not as pronounced as the increase in air flow velocity. The overall lowest h_{conv} value is about 55 W/m^{2}K at 25 km/h (for proportional rotational speed), and the highest approx. double that, 110 W/m^{2}K at 50 km/h (for the corresponding rotational speed being 3 times higher). Increase in rotational speed seems to have similar influence on increase of convective cooling for both designs, with fingered hub showing again better characteristics.

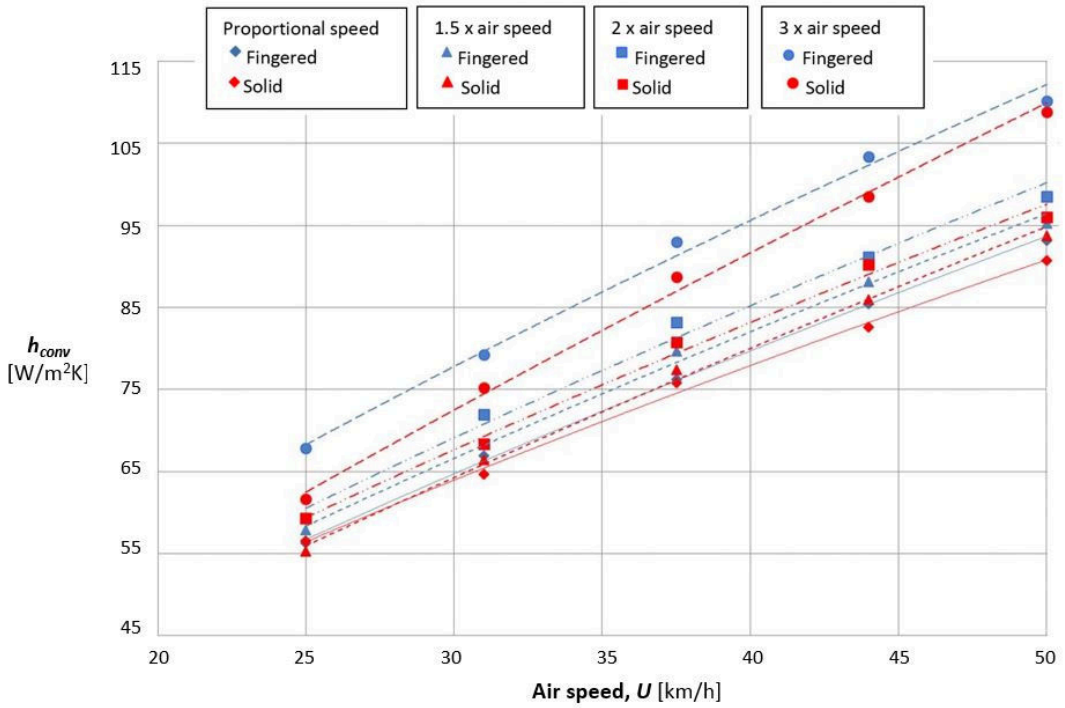

Figure 9 Change of the convective heat transfer coefficients for solid and fingered disc with air speed at 275°C for four rotational speeds

For the characterisation of the discs rotating in cross flow there are two Reynolds numbers and a three-dimensional graph in Figure 10 was used to plot Nusselt number as a function of the rotational Re_ω and the ratio Re_t / Re_ω.

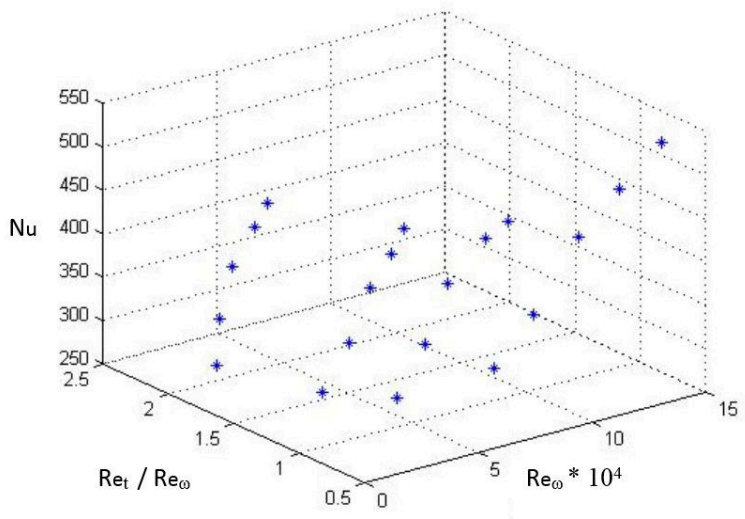

Figure 10 Nusselt number as a function of Re_ω and Re_t / Re_ω ratio

Although Figure 10 gives a reasonably good idea of the changes, it is actually of little practical use, therefore the terms *a*, *b* and *c* for the Equation (8) are graphically presented in Figure 11. Similarly to

the cooling in still air, solid hub disc shows more pronounced changes of terms *a* and *b* with increase in temperature, and now also for term *c*. The exception is the highest temperature (375°C), where all terms change quite substantially for the fingered design. The tests were repeated but the same results were obtained. The flows remain predominantly laminar for all conditions tested. At the maximum air velocity in the flow channel of 50 km/h (13.9 m/s), Re_t reaches 72,000 (for 125°C).

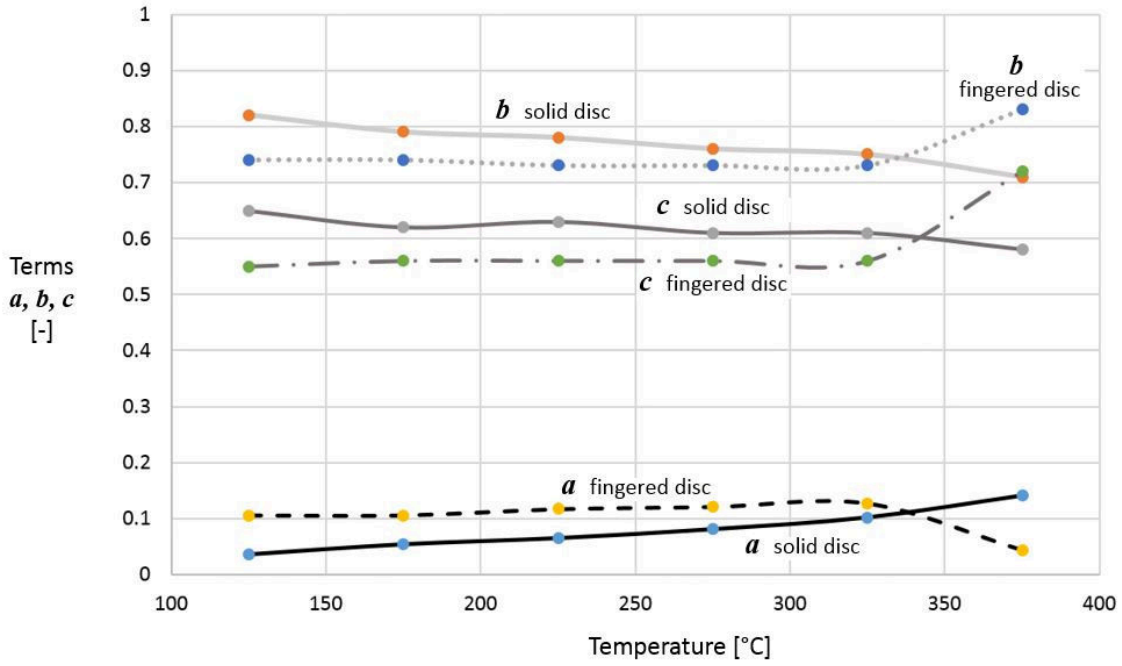

Figure 11 Cooling characterisation in cross flow: Terms ***a***, ***b*** and ***c*** for solid and fingered disc (Equation 8)

6. Discs rotating in a cross flow under angle

Disc rotating and heating assembly enables disc to rotate in an angle relative to the air flow within the flow channel. Figure 12 depicts such conditions, starting with 12a showing the parallel cross flow, studied in the previous section. Figure 12b illustrates +10° angle and 12c the angle of -10°. For reasons of brevity the results will be shown only for angles of -10° and +10°, though the Rig enables larger span of angles, between -28° and +25°. Different disc designs show different changes in cooling characteristics when subjected to angular flow. Depending on the disc design (type) and angular position, the air can be 'pushed' into the ventilation channels or 'deflected' from entering disc ventilations channels. The two distinctive automotive disc designs, standard and anti-coning, have air entry into the ventilation channels on opposite sides, which would lead to their different behaviour when subjected to angular flow. The discs studied here are of a standard but 'swan neck' type design (see Figure 1) and it would be expected for the angular test condition of +10° to facilitate better air entry into the ventilation channels of the solid disc, promoting heat dissipation from the vanes and channels.

As with all designs in such flow conditions, one disc face will be facing the flow and cooling better, with the other being in the 'shadow' and cooling worse. There is however fundamental difference between the discs studied, the fingered hub design would allow the flow to get through, whereas the solid hub should prevent the through flow, directing the air through the channels in +10° condition (Figure 12b) but blocking the flow in -10° (Figure 12c).

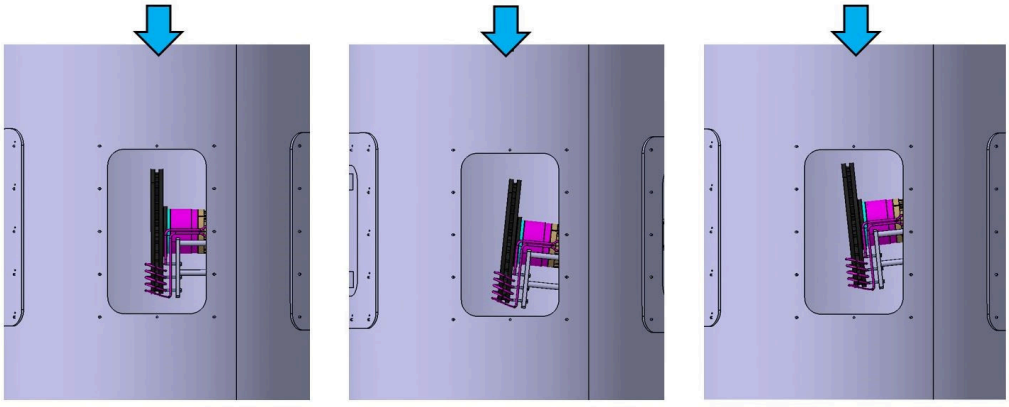

a) **b)** **c)**

Figure 12 Top view of the disc in the Flow channel (top hatch removed):
a) Parallel flow; **b)** +10° flow angle and **c)** -10° flow angle

For clarity reasons, only proportional speed condition results (in the form of convective heat transfer coefficients) are shown in Figure 13, again for 275°C. It is quite obvious that the flow +10° increases convective cooling in comparison with the parallel flow, in average by about 20% at 25 km/h reducing to about 10% at 50 km/h. The increase is more pronounced for the solid hub disc but the fingered design still exhibits superior heat dissipation characteristics, in particular at higher speeds. Contrary, at flow angle of -10° the cooling rates decrease, in particular for the solid hub disc. The reduction is nearly 20% at 25 km/h, and about 15% at 50 km/h. Fingered design demonstrates consistently better cooling throughout the speed range. As with parallel flow (presented in Section 5), 3D graphs can be created but they are of little practical use. In order to provide generic results, the terms *a*, *b* and *c* for the Equation (8) are presented in Figure 14 for the air flow angle of +10° and in Figure 15 for -10°.

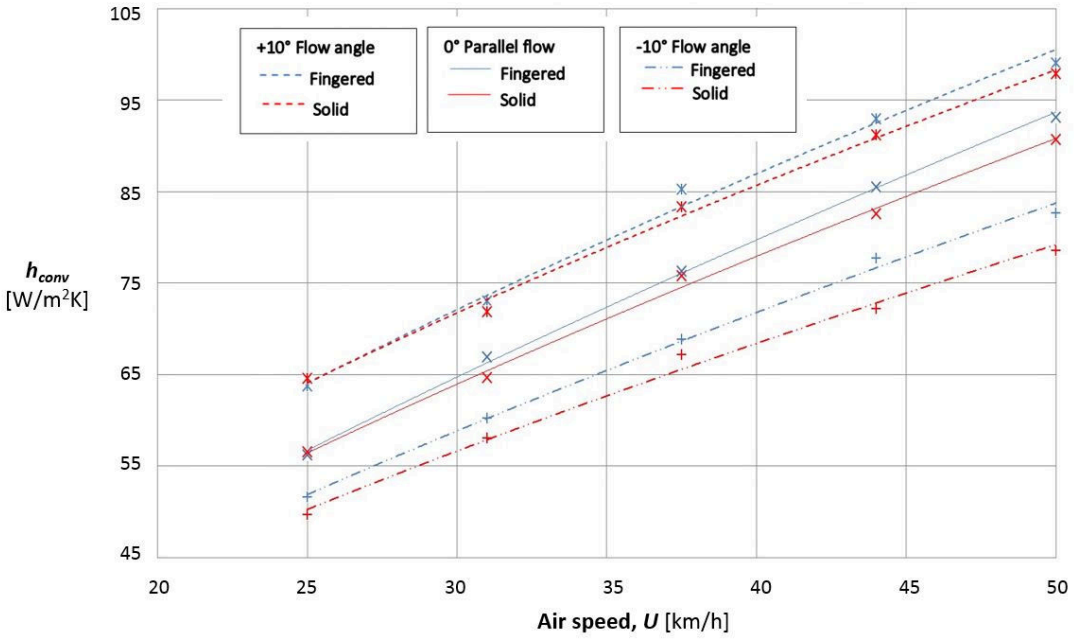

Figure 13 Change of the convective heat transfer coefficients for solid and fingered disc under angular cross flow with proportional air speed at 275°C

Similar to the rotation in still air and in parallel flow, solid hub disc shows somewhat more pronounced changes of terms *a* and *b* with increase in temperature for the +10° flow angle (Figure 14) but the changes are approximately linear. For the fingered design, terms *a* shows sudden drop at 375°C, with term *b* increasing. Term *c* remains fairly constant for both designs.

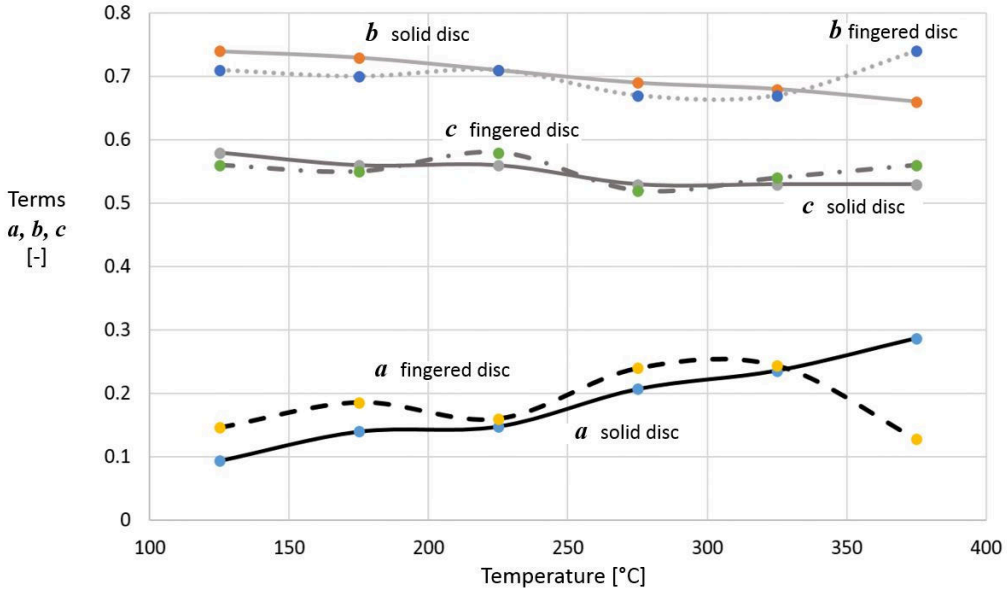

Figure 14 Cooling characterisation for +10° cross flow: Terms ***a***, ***b*** and ***c*** for solid and fingered disc (Equation 8)

For the cross flow at -10°, terms *a* and *b* show similar variations with temperature for both design to the previous case (+10°) but the changes are less pronounced. Term *c* changes little with temperature for the solid design but increases suddenly at the highest temperature (375°C) for the fingered design. The sudden changes at the highest temperature were investigated and cooling tests repeated several times (over a period of time) but the same results were consistently obtained.

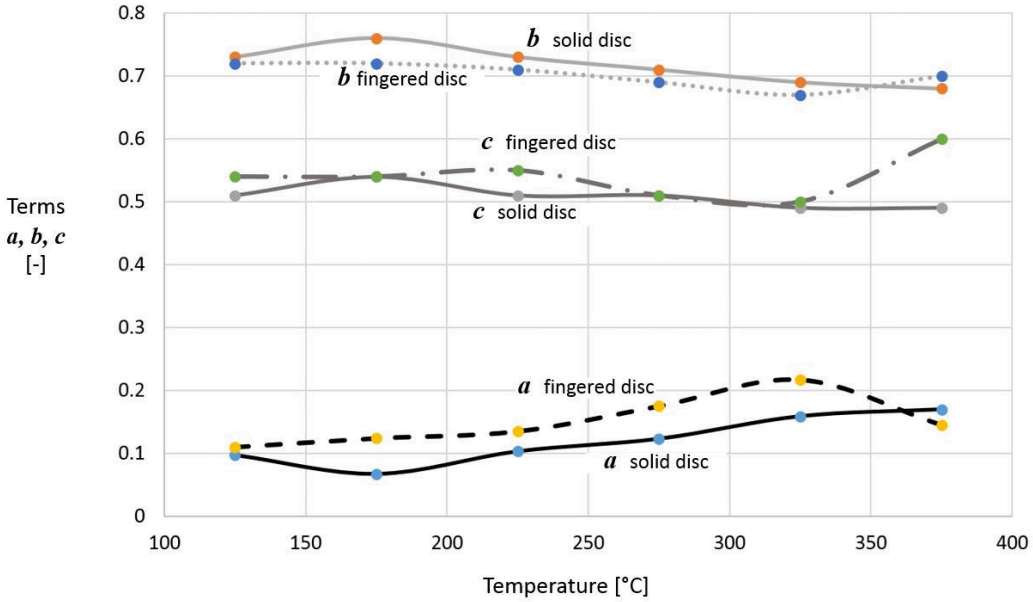

Figure 15 Cooling characterisation for -10° cross flow: Terms ***a***, ***b*** and ***c*** for solid and fingered disc (Equation 8)

In the addition to the above presented results, the tests were conducted for higher rotational speeds of 1.5, 2 and 3 times the corresponding air flow velocity. In all these conditions the fingered design showed superior cooling characteristics, with the gains summarised in Figure 16. The results are averaged over the temperature range, with the minimum gain being around 3.5% for proportional flow under +10° angle and maximum being 13.5% for 1.5 times rotational speed to air velocity ratio for flow angle of -10° angle.

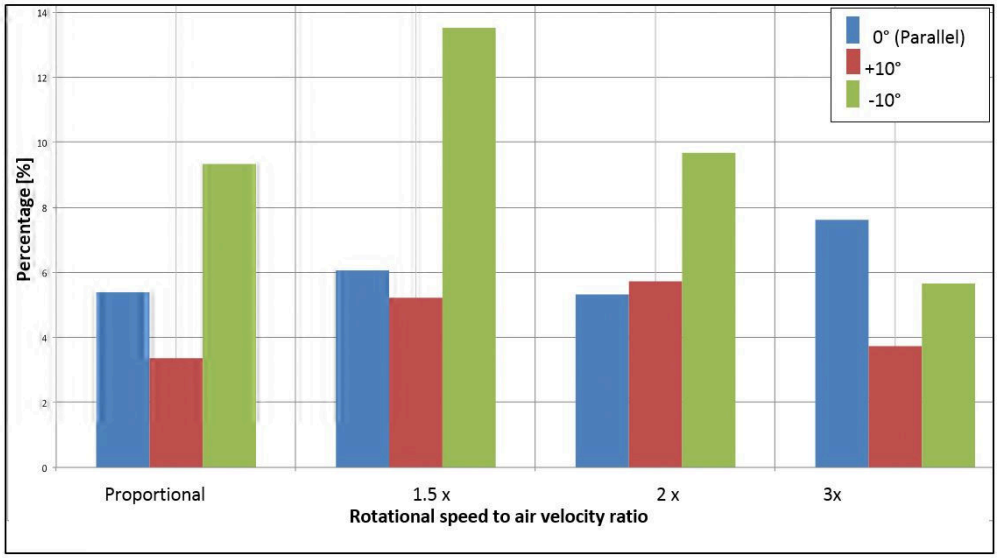

Figure 16 Fingered hub disc cooling improvement over solid design

7. Discussions and Conclusions

The Thermal Flow Rig developed proved to be a very valuable equipment. It is easy to operate, with the flow channel providing stable and uniform air flow and the heating and rotating assembly providing rapid and uniform disc heating up to 500°C. Disc design comparisons in terms of heat dissipation characteristics can be performed rapidly, accurately and at low cost. The results are generic, giving practical insight into suitability for vehicle installations and 'in vehicle tuning'.

The newly developed fingered hub design shows superior cooling characteristics to the standard, solid hub disc for all test conditions. The increase in the values of the average coefficient of convective heat dissipation varied depending on disc angular velocity, air flow speed and disc temperatures. At 275°C, when rotating in still air, the fingered disc convective cooling is higher by about 20%. When subjected to a cross flow, at proportional speed, the average increase is 5.3%, raising to 7.6% for triple speed.

The angular flow of +10° increases convective cooling in comparison with the parallel flow for both designs, in average by about 20% at 25 km/h reducing to about 10% at 50 km/h. The increase is more pronounced for the solid hub disc but the fingered design still exhibits superior heat dissipation characteristics, in particular at higher speeds. At flow angle of -10° the cooling rates decrease, especially for the solid hub disc, by nearly 20% at 25 km/h, and about 15% at 50 km/h. Fingered design demonstrates consistently better cooling all test conditions, between 3.5% and nearly 14%. All these analyses indicate that fingered design is more promising regarding 'in vehicle tuning' for improving convective cooling, as per Son et al. [19] the direction of air flow is most important for this effect, with the fingered design actively drawing air from both sides.

Comparisons using Nusselt and Reynolds numbers and associated parameters *a*, *b* and *c* showed to be the best method in obtaining the most generic results. These can be used to extract average convective heat transfer coefficients not only within the range of operating conditions tested but can be safely extrapolated. Furthermore, they can be also used for predicting cooling characteristics of similar design discs of different size.

Finally, new fingered design is 8.5% lighter when compared to the solid hub disc. Being a single piece cast design the manufacturing costs are low, offering a competitive product when compared to multi part discs which often do not offer such cooling improvements due to the complexity and limited space at disc inner diameter (caused by the flange/disc rotor joining mechanisms).

Acknowledgement

The generation of the initial fingered disc concept was partly supported by Eurac (Pool) Ltd Company as part of a different project and the authors are most grateful for this provision. Authors' particular thanks go to Dr David Eggleston and Mr Richard Sims for their input and support. With sadness and greatest respect the authors devote this paper in memory of Dr Eggleston. The Thermal Flow Rig was developed with support from Jaguar Land Rover, as part of a separate project. The authors are grateful for this support, in particular to Mr Daren Steward.

References

1. Topouris, S. and Tirovic, M., Design synthesis and structural optimization of a lightweight, monobloc cast iron brake disc with fingered hub. Journal of Engineering Optimisation, https://doi.org/10.1080/0305215X.2018.1542692.
2. Newcomb, T. P., Transient temperatures attained in disk brakes. British Journal of Applied Physics, 10(7), pp. 339-340, 1959.
3. Wagner, C., Heat transfer from a rotating disk to ambient air. Journal of Applied Physics, 19(9), pp. 837-839, 1948.
4. Cobb, E. C. and Saunders, O. A., Heat transfer from a rotating disk. Proceedings of the Royal Society of London A: Mathematical, Physical and Engineering Sciences, 236(1206), pp. 343-351, 1956.
5. Richardson, P. D. and Saunders, O. A., Studies of flow and heat transfer associated with a rotating disc. Journal of Mechanical Engineering Science, 5(4), pp. 336-342, 1963.
6. Noyes, R. N. and Vickers, P. T., Prediction of surface temperatures in passenger car disc brakes (No. 690457). SAE Technical Paper, 1969.
7. Morgan, S. and Dennis, R. W., A theoretical prediction of disc brake temperatures and a comparison with experimental data (No. 720090). SAE Technical Paper, 1972.

8. Limpert, R., Cooling analysis of disc brake rotors (No. 751014). SAE Technical Paper, 1975.
9. Sisson, A. E., Thermal analysis of vented brake rotors (No. 780352). SAE Technical Paper, 1978.
10. Dufrenoy, P., Berte, E., Witz, J-F. and Desplanques, Y., A New Camera for Quantitive Measurements of Temperature and Emissivity During Braking, Paper EB2018-VDT-033, EuroBrake Conference, 22-24 May 2018, The Hague, Netherlands,
11. Moffat, R., Describing the uncertainties in experimental results. Experimental Thermal and Fluid Science, 1(1), pp. 3-7, 1988.
12. Grieve, D. G., Barton, D. C., Crolla, D. A. and Buckingham, J. T., Design of a lightweight automotive brake disc using finite element and Taguchi techniques. Proceedings of the Institution of Mechanical Engineers, Part D: Journal of Automobile Engineering, 212(4), pp. 245-254, 1998.
13. Tang, J., Bryant, D. and Qi, H., Experimental Investigation of the Dynamic Thermal Deformation and Judder of a Ventilated Disc Brake, Paper EB2018-FBR-002, EuroBrake Conference, 22-24 May 2018, The Hague, Netherlands.
14. Stevens, K., An Investigation into Heat Dissipation from a Stationary Commercial Vehicle Brake Disc in Parked Conditions - EngD Thesis, Cranfield University, 2013.
15. Stevens K. and Tirovic M., Heat dissipation from a stationary brake disc, Part 1: Analytical modelling and experimental investigations, Proc IMechE Part C: J Mechanical Engineering Science, Vol. 232(9) 1707–1733, 2018.
16. Tirovic, M. and Voller, G.P., Interface pressure distributions and thermal contact resistance of a bolted joint, Proceedings of The Royal Society, Series A (2005) 461, pp. 2339-2354.
17. Teimourimanesh S., Vernersson, T. and Lunden, R., Modelling of temperatures during railway tread braking: Influence of contact conditions and rail cooling effect. Proc. Instn. Mech. Engrs. Part F, Journal of Rail and Rapid Transit, Vol. 228 (1) 93-109, 2014.
18. Topouris, S. Design and Optimisation of a High Performance Lightweight Monoblock Cast Iron Brake Disc, PhD Thesis, Cranfield University, 2017.
19. Son, J.K., Jung Y-S. and Jeon, H-h., Optimization Analysis and Design of Brake Cooling System, Paper EB2018-SVM-003, EuroBrake Conference, 22-24 May 2018, The Hague, Netherlands.

Experimental investigation of the cooling characteristics of a monobloc cast iron brake disc with fingered hub

Tirovic, Marko

2019-05-02

Tirovic M, Topouris S, Sherwood G. (2020) Experimental investigation of the cooling characteristics of a monobloc cast iron brake disc with fingered hub. Proceedings of the Institution of Mechanical Engineers, Part D: Journal of Automobile Engineering, Volume 234, Issue 1, January 2020, pp. 85-97

https://doi.org/10.1177/0954407019838642